Available online at www.sciencedirect.com
ScienceDirect
Journal of Sound and Vibration 312 (2008) 726–735
JOURNAL OF SOUND AND VIBRATION
www.elsevier.com/locate/jsvi

On the use of the auto-bispectral density for detecting quadratic nonlinearity in structural systems

J.M. Nichols[a,*], P. Marzocca[b], A. Milanese[b]

[a]*Naval Research Laboratory, 4555 Overlook Ave., Washington, DC 20375, USA*
[b]*Department of Mechanical and Aeronautical Engineering, Clarkson University, Potsdam, NY 13699-5725, USA*

Received 19 June 2007; received in revised form 26 October 2007; accepted 7 November 2007
Available online 31 December 2007

Abstract

Higher-order spectra appear often in the analysis and identification of nonlinear systems. The auto-bispectral density is one example of a higher-order spectrum and may be used in the analysis of stationary structural response data to detect the presence of certain types of structural nonlinearities. In this work a closed-form expression for the auto-bispectral density, derived previously by the authors, is used to find the bispectral frequency most sensitive to the nonlinearity. The properties of nonlinearity detectors based on estimates of the magnitude of the auto-bispectral density at this frequency are then explored. Estimates of the auto-bispectral density are obtained using the direct method based on the discrete Fourier transform. The bias associated with this estimator is derived here and combined with previously derived expressions for the estimator variance to give both Type-I and Type-II errors for the detector. Detector performance is quantified using a receiver operating characteristic (ROC) curve illustrating the trade-off between false positives (Type-I error) and power of detection (1.0-Type-II error). Theoretically derived ROC curves are compared to those obtained via numerical simulation and show excellent agreement. Results are presented for different levels of nonlinearity in both the stiffness and damping terms for a spring–mass system. Possible consequences are discussed with regard to the detection of damage-induced nonlinearities in structures.
Published by Elsevier Ltd.

1. Introduction

This work is concerned with detecting the presence of certain kinds of nonlinearity in structural systems. Specifically, nonlinearity detectors based on estimates of the auto-bispectral density obtained from time series of structural response data are considered. The auto-bispectral density for a stationary system response is defined as the double Fourier transform (FT) of the third moment about the mean [1], i.e.

$$B(\omega_1,\omega_2)=\int_{-\infty}^{\infty}\int_{-\infty}^{\infty}E[(y(t)-\bar{y})(y(t+\tau_1)-\bar{y})(y(t+\tau_2)-\bar{y})]e^{-i(\omega_1\tau_1+\omega_2\tau_2)}\,d\tau_1\,d\tau_2, \quad (1)$$

where $y(t)$ is the signal and $\bar{y}$ is the signal mean. The distinction is sometimes not made between the terms "auto-bispectrum" and "auto-bispectral density". Eq. (1) is in fact a density with units $[y]^3/\mathrm{Hz}^2$ and will be

*Corresponding author. Tel.: +1 202 404 5433; fax: +1 202 767 5792.
E-mail address: jonathan.nichols@nrl.navy.mil (J.M. Nichols).

0022-460X/$ - see front matter Published by Elsevier Ltd.
doi:10.1016/j.jsv.2007.11.032

referred to as such throughout. The expected value under the integral will only be a function of the delays τ_1, τ_2 due to the assumption of ergodicity. For a linear Gaussian-excited structure this quantity is zero for all frequency pairs ω_1, ω_2. This can be seen as follows. Assume a linear, time invariant system driven with zero-mean Gaussian noise $x(t)$. Its input–output relationship is governed by the convolution

$$y(t) = \int_{-\infty}^{\infty} h(\tau)x(t-\tau)\,\mathrm{d}\tau \tag{2}$$

and the statistical moments of the output are given by $E[y(t)] = E[x(t)] = 0$ followed by

$$\begin{aligned} E[y(t)y(t+\tau_1)] &= \int_{-\infty}^{\infty}\int_{-\infty}^{\infty} h(t-\theta_1)h(t+\tau_1-\theta_2)E[x(\theta_1)x(\theta_2)]\,\mathrm{d}\theta_1\,\mathrm{d}\theta_2, \\ E[y(t)y(t+\tau_1)y(t+\tau_2)] &= \int_{-\infty}^{\infty}\int_{-\infty}^{\infty}\int_{-\infty}^{\infty} h(t-\theta_1)h(t+\tau_1-\theta_2)h(t+\tau_2-\theta_3) \\ &\quad \times E[x(\theta_1)x(\theta_2)x(\theta_3)]\,\mathrm{d}\theta_1\,\mathrm{d}\theta_2\,\mathrm{d}\theta_3 \\ &\vdots \end{aligned} \tag{3}$$

Because the excitation is Gaussian all odd-order moments vanish, e.g. $E[x(\theta_1)x(\theta_2)x(\theta_3)] = 0$, while the even order expectations become functions of the autocovariance $E[x(\theta_1)x(\theta_2)]$ [2]. As a consequence the statistical properties of the output for a linear, Gaussian driven system can be described entirely by $E[y(t)y(t+\tau_1)]$ (e.g. $E[y(t)y(t+\tau_1)y(t+\tau_2)] = 0$). However, if quadratic nonlinearities are present, Eq. (2) does not hold and there will exist non-zero components in the third moment, i.e. $E[y(t)y(t+\tau_1)y(t+\tau_2)] \neq 0$. The presence of this expected value can therefore be used to infer the presence of the nonlinearity. The existence of other higher-order moments can also be used to detect nonlinearity for Gaussian driven linear structures. The frequency domain representations of these moments are collectively the higher-order spectra. The first of these, the auto-bispectral density has already been given by Eq. (1) and is the focus of this work. Even if the excitation, $x(t)$, is non-Gaussian a normalized form of Eq. (1), the bicoherence, can be used to detect the presence of a nonlinearity [3]. In this case the practitioner is trying to detect deviations from a constant bicoherence as opposed to non-zero values as is done with the auto-bispectral density.

The magnitude of the auto-bispectrum has seen use as a nonlinearity detector in a number of applications. Worden and Tomlinson [4] used estimates of the auto-bispectrum to detect different types of nonlinearity in a spring–mass system. Messina and Vittal [5] used estimates of the auto-bispectrum to detect nonlinear mode interaction in a power system. In some cases structural damage will result in the presence of a nonlinearity. Rivola and White [6] used the normalized auto-bispectrum to detect cracks in an experimental beam while Zhang et al. [7] focused on detecting gear faults, also using the auto-bispectrum. Both the auto-bispectrum and auto-trispectrum were used by Teng and Brandon [8] in detecting the deterioration of jointed structures. One question that was not addressed in the above works was that of significance. That is to say, what are the Type-I and Type-II errors associated with a bispectral-based detector? In detecting the presence of non-Gaussian signals in noise, Hinich and Wilson [9] specified both Type-I and Type-II error as a function of both signal-to-noise-ratio (SNR) and the degree of non-normality (skewness). Type-I error was also discussed in the work of Richardson and Hodgkiss [1] in detecting nonlinearity in underwater acoustic data. To date no such analysis has been performed with regard to detecting nonlinearity in structures. However, this information is essential in understanding the efficacy of bispectrum-based detectors in applications such as damage detection mentioned above.

This work is focused on determining the Type-I and Type-II error for a detector of structural nonlinearity based on estimates of the auto-bispectral density. Determination of these errors first requires an analytical solution for the auto-bispectral density as a function of the nonlinearity parameters. Such a solution was previously derived by the authors in Ref. [10] and is summarized in the next section. This solution is also used to determine the frequency pair (ω_1, ω_2) most sensitive to the presence of the nonlinearity. The bias associated with the direct method of estimating the auto-bispectral density is then derived. This expression is used in conjunction with previously established expressions for the variance of the estimator to derive the distributions for the magnitude auto-bispectral density peak heights under the null (linear) and alternative

(nonlinearity present) hypothesis. Probability of detection (1.0-Type-II error) and probability of false alarm (Type-I error) can then be obtained analytically for a given nonlinearity strength. These results are displayed as receiver operating characteristic (ROC) curves and are compared to those obtained by simulating the nonlinear response of a spring–mass system and subsequently estimating the auto-bispectral density.

2. Analytical auto-bispectral density via Volterra series

This section briefly reviews the development of an analytical solution for the auto-bispectral density and shows how this solution can be used to obtain the most sensitive bi-frequency for the purposes of nonlinearity detection. In order to describe the output response analytically a two-term Volterra series model is used [2,11] in which the solution is approximated as

$$\begin{aligned} y(t) &= y_1(t) + y_2(t) \\ &= \int_{-\infty}^{\infty} h_1(\tau)x(t-\tau)\,\mathrm{d}\tau + \int_{-\infty}^{\infty}\int_{-\infty}^{\infty} h_2(\tau_1,\tau_2)x(t-\tau_1)x(t-\tau_2)\,\mathrm{d}\tau_1\,\mathrm{d}\tau_2, \end{aligned} \tag{4}$$

where h_1, h_2 are the linear and quadratic Volterra kernels, respectively. This approach is valid for modeling a broad class of nonlinear systems (see Ref. [2]). While more terms could have been considered in the Volterra expansion (e.g. $y_3(t)$, $y_4(t)$, etc.), the focus of this work is on establishing detection limits (i.e. relatively low levels of nonlinearity are considered). For this application the two term model is sufficient. Consider the excitation to be IID Gaussian noise with zero mean and unit standard deviation, i.e. $x(t)\sim N(0,1)$. In this case the mean of the system response is given by

$$\bar{y} = \bar{y}_1 + \bar{y}_2 = 0 + \int_{-\infty}^{\infty}\int_{-\infty}^{\infty} h_2(\tau_1,\tau_2)E[x(t-\tau_1)x(t-\tau_2)]\,\mathrm{d}\tau_1\,\mathrm{d}\tau_2. \tag{5}$$

Substituting Eqs. (4) and (5) into Eq. (1) and simplifying yields the expression [10]

$$\begin{aligned} &B(\omega_1,\omega_2) \\ &= \frac{8}{2\pi}\int_{-\infty}^{\infty} H_2(\omega_1+\xi,\omega_2-\xi)H_2(-\omega_1-\xi,\xi)H_2(-\omega_2+\xi,-\xi)S_{xx}(\xi)S_{xx}(\omega_1+\xi)S_{xx}(\omega_2-\xi)\,\mathrm{d}\xi \\ &\quad + 2H_2(-\omega_1-\omega_2,\omega_2)H_1(\omega_1+\omega_2)H_1(-\omega_2)S_{xx}(\omega_1+\omega_2)S_{xx}(\omega_2) \\ &\quad + 2H_2(-\omega_1-\omega_2,\omega_1)H_1(\omega_1+\omega_2)H_1(-\omega_1)S_{xx}(\omega_1+\omega_2)S_{xx}(\omega_1) \\ &\quad + 2H_2(\omega_1,\omega_2)H_1(-\omega_1)H_1(-\omega_2)S_{xx}(\omega_1)S_{xx}(\omega_2), \end{aligned} \tag{6}$$

where $S_{xx}(\omega) = \int_{-\infty}^{\infty} E[x(t)x(t-\tau_1)]\mathrm{e}^{-\mathrm{i}\omega\tau_1}\,\mathrm{d}\tau_1$ is the autospectral density function. In this work the IID Gaussian assumption on $x(t)$ results in $S_{xx}(\omega) = \text{const.} = P$. Expressions for the frequency domain kernels, $H_1(\omega) = \int_{-\infty}^{\infty} h_1(\tau_1)\mathrm{e}^{-\mathrm{i}\omega\tau_1}\,\mathrm{d}\tau_1$ and $H_2(\omega_1,\omega_2) = \int_{-\infty}^{\infty}\int_{-\infty}^{\infty} h_2(\tau_1,\tau_2)\mathrm{e}^{-\mathrm{i}(\omega_1\tau_1+\omega_2\tau_2)}\,\mathrm{d}\tau_1\,\mathrm{d}\tau_2$, may be obtained via the harmonic probing technique described in detail in Refs. [11,12]. These kernels will be dependent on the specific system under study.

Define the structural model of interest to be a single degree-of-freedom system governed by

$$m\ddot{y} + c_1\dot{y} + c_2\dot{y}^2 + k_1 y + k_2 y^2 = Ax(t), \tag{7}$$

where m [kg] is the mass, c_1 [N s/m] and k_1 [N/m] the linear damping and stiffness coefficients, c_2 [N s^2/m^2] and k_2 [N/m^2] the nonlinear damping and stiffness coefficients, and A [N] the amplitude of excitation. Using the acceleration $\ddot{y}(t)$ as the response of interest, harmonic probing yields

$$H_1(\omega) = \frac{-\omega^2}{k_1 + \mathrm{i}c_1\omega - m\omega^2}$$

$$H_2(\omega_1,\omega_2) = \frac{1}{\omega_1^2\omega_2^2}(-k_2 + c_2\omega_1\omega_2)H_1(\omega_1)H_1(\omega_2)H_1(\omega_1+\omega_2) \tag{8}$$

as the first and second-order Volterra kernels. These expressions may be substituted into Eq. (6) along with $S_{xx}(\omega) = P[\mathrm{N}^2/\mathrm{Hz}]$ to give a closed-form solution for the auto-bispectral density in terms of the physical parameters m, k_1, k_2, c_1, c_2. The integral term of Eq. (6) may be obtained via Cauchy integration (see for example Ref. [13]). For a Gaussian excited, linear structure $H_2(\omega_1, \omega_2) = 0$ ($k_2 = c_2 = 0$) and the auto-bispectral density is identically zero over all frequency pairs. For the system studied here, the presence of a nonlinearity in either the damping or stiffness terms will lead to non-zero values resulting in "peaks" at both the natural frequency $\omega_n = \sqrt{k_1/m}$ and the bi-frequency $\omega_1 + \omega_2 = \omega_n$. This can be seen simply by considering the location of the poles associated with $H_2(\omega_1, \omega_2)$ (see Fig. 1). Differentiating Eq. (6) with respect to k_2 or c_2 shows that the peak location $\omega_1 = \omega_2 = \omega_n$ is clearly the most sensitive to the presence of both stiffness and damping nonlinearities. The analytical expression is also needed in order to derive the distributions for the magnitude auto-bispectral density peak heights. Detecting the presence of these nonlinearities therefore requires the practitioner to monitor this frequency pair in the ω_1, ω_2 plane and look for significant non-zero values. In the following sections we discuss the estimation problem and the problem of determining the significance of the magnitude auto-bispectral density peak heights.

3. Estimating the auto-bispectral density

The estimation of $B(\omega_1, \omega_2)$ is made with finite data and will therefore be subject to both bias and variance. This results in non-zero values of the bispectrum even when no nonlinearity is present. Ideally, the estimator used will be unbiased and consistent, that is to say both the bias and variance will go to zero as the number of data points become large. The real question for detection is "what is the smallest nonlinearity that can be detected with a given Type-I, Type-II error given the uncertainty in the estimate?". Of course, other noise sources will be present in practice and will degrade the detection performance further. By considering only the uncertainty in the estimate, the results presented show the fundamental limitations of this detection scheme.

Two main approaches are used in bispectral density estimation. The first, referred to as the *indirect method*, involves averaging over K data records to approximate the expected value $E[(y(t) - \bar{y})(y(t - \tau_1) - \bar{y})(y(t - \tau_2) - \bar{y})]$ and then taking the double FT. Details of this approach are discussed in Ref. [14]. The second, *direct method* forms the estimate as an average product of FTs. An observed time series sampled with frequency $f_s = 1/\Delta_t$ is denoted $y(n), n = 0 \cdots N - 1$. These data are divided into K segments of length M ($N = KM$ for non-overlapping segments) such that the kth segment is $y_k(m) = y(m + kM), m = 0 \cdots M - 1, k = 0 \cdots K - 1$. Each segment may then be smoothed by multiplying by an appropriate windowing function $w(m)$. The FT of the windowed data at discrete frequencies f is approximated by $Y_k(f) = \Delta_t \sum_m w(m) y_k(m) \mathrm{e}^{-\mathrm{i}2\pi fm/M}$, $f = 0, \ldots, M - 1$. Using this notation, the final estimate for the auto-bispectral density is obtained by averaging over the total time $KM\Delta_t$ to give

$$\hat{B}(f, g) = \frac{\Delta_t^2}{KM} \sum_{k=0}^{K-1} Y_k(f)\, Y_k(g)\, Y_k^*(f + g) \tag{9}$$

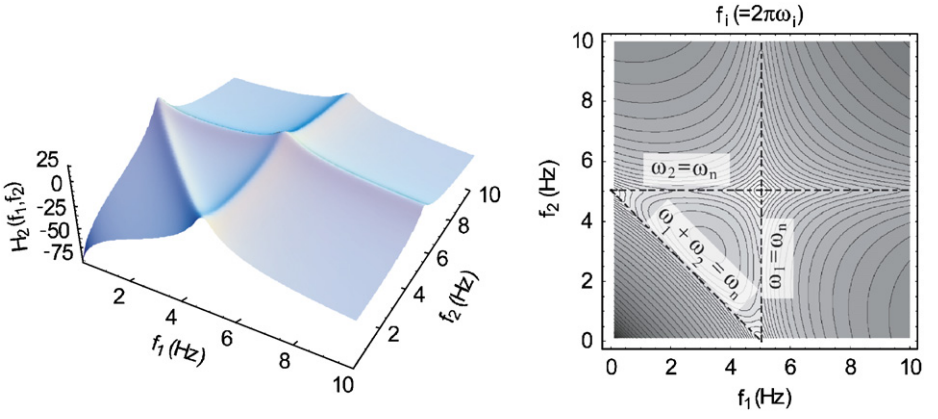

Fig. 1. Magnitude of $H_2(\omega_1, \omega_2)$ (dB scale) showing the location of the poles and the ridge $\omega_1 + \omega_2 = \omega_n$.

for discrete frequencies f, g. Obtaining the estimate at frequencies (ω_1, ω_2) simply requires the scaling $\omega = 2\pi[(2f - M)/2M\Delta_t], f = 0 \cdots M - 1$ resulting in the estimate $\hat{B}(\omega_1, \omega_2)$.

As the number of data increases toward infinity, the bias in the estimate approaches zero, thus Eq. (9) is an unbiased estimate [14]. The bias in bispectral estimates is analogous to that found in power spectrum estimation and scales as the second derivative of the auto-bispectral density with respect to the frequencies [15]. For lightly damped systems, such as the mechanical system explored here, there will tend to be sharp peaks such as the one displayed in Fig. 2 resulting in a potentially large bias. Accurate resolution of sharp peaks requires a high-frequency resolution. This means that the number of points in the estimation segments M must be large. An estimate for the bias is derived here in analogous fashion to those derived in power spectral density estimation [16]. The expected value for the estimate may be written as the value of the magnitude auto-bispectral density averaged over each frequency bin, i.e.

$$E[|\hat{B}(f_1,f_2)|^2] = \frac{1}{(2\Delta_f)^2}\int_{f_2-\Delta_f}^{f_2+\Delta_f}\int_{f_1-\Delta_f}^{f_1+\Delta_f} |\hat{B}(\xi_1,\xi_2)|^2\,\mathrm{d}\xi_1\,\mathrm{d}\xi_2. \tag{10}$$

where $\Delta_f = 1/(2M\Delta_t)$ is the half-frequency bin width. For small Δ_f, the magnitude auto-bispectral density may be expanded as a Taylor series up to second order giving

$$\begin{aligned} E[|\hat{B}(f_1,f_2)|^2] \approx \frac{1}{(2\Delta_f)^2}\int_{f_2-\Delta_f}^{f_2+\Delta_f}\int_{f_1-\Delta_f}^{f_1+\Delta_f} & |\hat{B}(f_1,f_2)|^2 + (\xi_1 - f_1)\frac{\partial}{\partial f_1}|\hat{B}(f_1,f_2)|^2 \\ & + (\xi_2 - f_2)\frac{\partial}{\partial f_2}|\hat{B}(f_1,f_2)|^2 + (\xi_1 - f_1)(\xi_2 - f_2)\frac{\partial^2}{\partial f_1 \partial f_2}|\hat{B}(f_1,f_2)|^2 \\ & + \frac{1}{2}(\xi_1 - f_1)^2\frac{\partial^2}{\partial f_1^2}|\hat{B}(f_1,f_2)|^2 + \frac{1}{2}(\xi_2 - f_2)^2\frac{\partial^2}{\partial f_2^2}|\hat{B}(f_1,f_2)|^2\,\mathrm{d}\xi_1\,\mathrm{d}\xi_2. \end{aligned} \tag{11}$$

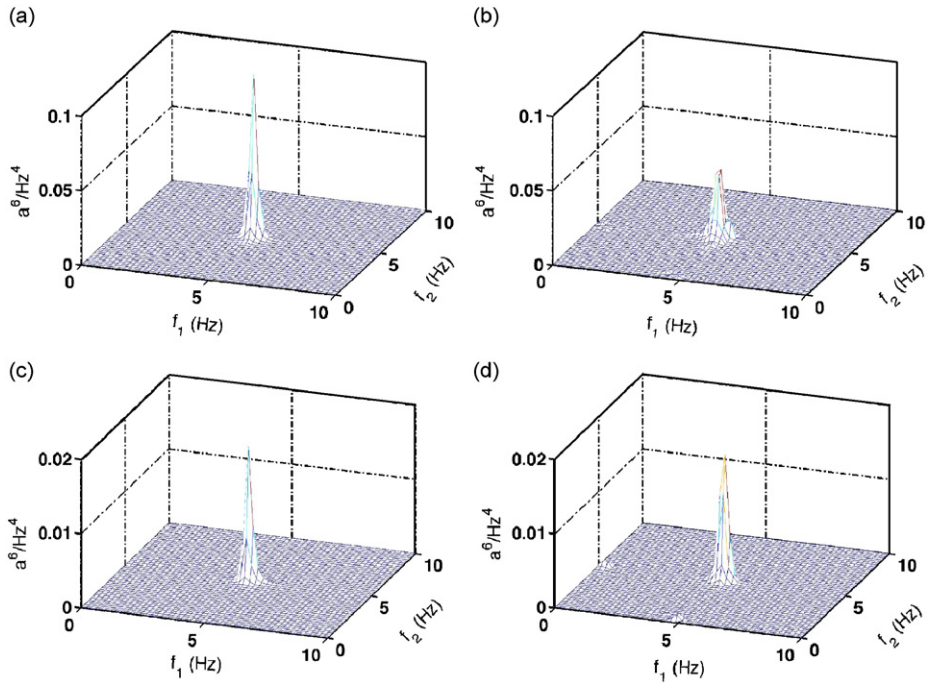

Fig. 2. Magnitude auto-bispectral density obtained from theory (a,c) and from the direct estimation procedure (b,d). Results are plotted for a stiffness nonlinearity of $k_2 = 10^5\,\mathrm{N/m^2}$, with $c_2 = 0\,\mathrm{N\,s^2/m^2}$ (a,b) and damping nonlinearity of $c_2 = 40\,\mathrm{N\,s^2/m^2}$ with $k_2 = 0\,\mathrm{N/m^2}$ (c,d).

The two terms involving the first derivative of the auto-bispectral density vanish as does the mixed partial derivative owing to the fact that $\int_{f-\Delta_f}^{f+\Delta_f}(\xi-f)\,\mathrm{d}\xi=0$. Carrying out the integration for the remaining terms results in the expression

$$E[|\hat{B}(f_1,f_2)|^2]\approx|B(f_1,f_2)|^2+\frac{\Delta_f^2}{6}\frac{\partial^2}{\partial f_1^2}|B(f_1,f_2)|^2+\frac{\Delta_f^2}{6}\frac{\partial^2}{\partial f_2^2}|B(f_1,f_2)|^2 \tag{12}$$

thus the bias is simply

$$b=\frac{\Delta_f^2}{6}\frac{\partial^2}{\partial f_1^2}|B(f_1,f_2)|^2+\frac{\Delta_f^2}{6}\frac{\partial^2}{\partial f_2^2}|B(f_1,f_2)|^2. \tag{13}$$

Using the closed-form expression for the auto-bispectral density (Eq. (6)) in combination with Eq. (13) an expression for the bias is obtained. One point of interest regarding Eq. (13) concerns the scaling with the nonlinearity parameters c_2, k_2. The bias term grows proportional to the size of the nonlinearity squared, i.e. $b\sim k_2^2, c_2^2$. Thus, for linear increases in the nonlinearity strength, quadratic increases in the bias are expected. Additionally, it is evident that the bias also scales as $1/M^2$, thus a linear increase in frequency resolution provides a large reduction in bias. However, as will be shown next, for a consistent estimate of the auto-bispectral density there exists a rather severe constraint on allowable M.

The variance associated with this estimate has already been derived [17,18]. For non-overlapping data segments and no windowing the cited works have shown that both the real and imaginary parts of $\hat{B}(\omega_1,\omega_2)$ are asymptotically Gaussian distributed with common variance given by

$$\sigma^2=\sigma_{\mathrm{Re}}^2=\sigma_{\mathrm{Im}}^2=\frac{1}{2}\frac{M^2\Delta_t}{N}S_{yy}(\omega_1)S_{yy}(\omega_2)S_{yy}(\omega_1+\omega_2) \tag{14}$$

for all non-diagonal frequency pairs ($\omega_1\neq\omega_2$) while the variance is doubled ($\sigma^2\to 2\sigma^2$) for frequencies on the diagonal ($\omega_1=\omega_2$) [18]. In the absence of any bias, the means of these distributions are given by $E[\mathrm{Re}\{\hat{B}(\omega_1,\omega_2)\}]=\mathrm{Re}\{B(\omega_1,\omega_2)\}$ and $E[\mathrm{Im}\{\hat{B}(\omega_1,\omega_2)\}]=\mathrm{Im}\{B(\omega_1,\omega_2)\}$, respectively, for which we have analytical expressions. From Eq. (14) it is seen that for a consistent estimate the number of data points used in each segment must fulfill $M<N^{1/2}$. Using windowed, overlapping segments can help ease this constraint but the scaling of M with N remains. As with the estimation of power spectra there is clearly a trade-off between bias and variance. It should be mentioned that the auto-spectral density $S_{yy}(\omega)$ used in Eq. (14) contains an additional term due to the nonlinearity. The full expression, assuming a second-order Volterra model with an input spectrum $S_{xx}(\omega)=P$, was found to be

$$S_{yy}(\omega)=P|H_1(\omega)|^2+2P^2\int_{-\infty}^{\infty}|H_2(\omega_1,\omega-\omega_1)|^2\,\mathrm{d}\omega_1. \tag{15}$$

This expression was also simplified via Cauchy integration and is given by

$$\begin{aligned}S_{yy}(\omega)&=P|H_1(\omega)|^2\\&\quad+\frac{2\pi P^2\{[\omega_n^2c_2^2\omega^4+(-3c_2^2\omega_n^4-6c_2k_2\omega_n^2+k_2^2)\omega^2+4\omega_n^2(c_2\omega_n^2+k_2)^2]m^2+c_1^2(\omega_n^2\omega^2c_2^2+4k_2^2)\}}{m\omega_n^2c_1(m^2\omega^2+c_1^2)[m^2(\omega^2-4\omega_n^2)^2+4\omega^2c_1^2]}\\&\quad\times|H_1(\omega)|^2.\end{aligned} \tag{16}$$

The second term of Eq. (16) is higher-order $O(P^2)$ and therefore does not contribute significantly to the auto-bispectral density variance. It is included here for completeness. The detector used in this work is based on the magnitude of the auto-bispectral density squared, i.e. $|B(\omega_1,\omega_2)|^2=\mathrm{Re}[B(\omega_1,\omega_2)]^2+\mathrm{Im}[B(\omega_1,\omega_2)]^2$. The distribution for the sum of the squares of two Gaussian random variables with the same variance, but different means can be shown to be non-central, χ^2 with two statistical degrees-of-freedom and is given by [19]

$$p(s)=\tfrac{1}{2}e^{-(s+\lambda)/2}I_0(\sqrt{s\lambda}), \tag{17}$$

where $s=|\hat{B}(\omega_1,\omega_2)|^2/\sigma^2$, $\lambda=(|B(\omega_1,\omega_2)|^2-b)/\sigma^2$ is the non-centrality parameter and I_0 is the modified Bessel function of the first kind.

In the case of no nonlinearity ($\lambda = 0$) the Bessel function evaluates to unity and Eq. (17) reduces to the central χ^2 distribution with two degrees-of-freedom, i.e. the null distribution. The alternative is that there is a nonlinearity resulting in a non-zero $B(\omega_1, \omega_2)$ for which an analytical solution is known from the previous section. With both the null and the alternative distributions a complete accounting of the Type-I and Type-II errors is possible. In the next section, some results are presented showing the performance of the auto-bispectral density-based detector using the direct method of estimation. The detection of nonlinearity for both the damping ($c_2 \neq 0$) and stiffness ($k_2 \neq 0$) terms is considered.

4. Detector performance

Detector performance will be quantified using ROC curves [19]. In problems of detection, the ROC curve provides a convenient means of displaying both Type-I and Type-II errors. The practitioner simply plots the probability of detection (POD, or 1.0-Type-II error) vs. the probability of false alarm (PFA) as the detection threshold is varied. As the threshold is raised the Type-I error is decreased, however this will typically cause a reduction in the POD. A low detection threshold gives a high POD but results in greater numbers of false positives. The ideal detector, of course, is one that minimizes both Type-I and Type-II error, i.e. maintains a high POD for a low PFA. The decision as to whether a given detector is implemented depends on the costs associated with Type-I and Type-II error. Different applications will undoubtedly have different requirements in this respect. Without knowledge of these costs the best that can be done is to display the detection probabilities for which the ROC curve is an appropriate tool.

The system given by Eq. (7) was integrated using the Euler–Maruyama scheme. This approach is appropriate for stochastic differential equations and will preserve the correct output variance [10]. The parameters for the linear system were fixed to the values $m = 1.0$ [kg], $k_1 = 10^3$ [N/m], $c_1 = 3.0$ [N s/m] with a sampling interval of $\Delta_t = 0.01$ s. The nonlinear system parameters, c_2 [N s^2/m^2] and k_2 [N/m^2] were varied in order to understand their effects on the system response. For the auto-bispectral density estimates the time series length was fixed to $N = 32,768$ points while the window size was chosen to be $M = 128$.

Fig. 2 shows both theoretical and estimated magnitude bispectral densities obtained for both stiffness (top row) and damping (bottom row) nonlinearities. The presence of the nonlinearity results in the peak observed at the system natural frequency. In the absence of the nonlinearity this peak disappears.

The detection problem involves discerning the Type-I and Type-II error associated with declaring a peak present. The magnitude auto-bispectral density peaks of Fig. 2 are clearly visible thus a POD of nearly unity would be expected for nearly zero PFA. However, as the degree of nonlinearity decreases it becomes more difficult to distinguish these peaks from the fluctuations present in the estimate. As was stated earlier, in this work the uncertainty is simply given by the error in the integration routine (not accounted for in the theory but assumed negligible) and the estimation error (which is accounted for in the theory).

The goal of this section is to explore the limitations in detecting both stiffness and damping nonlinearities. To this end the expected distributions for the magnitude auto-bispectral density peak height as a function of both c_2, k_2 was analytically obtained. The distributions were also obtained numerically by simulating 40 realizations of the random process described by Eq. (7). A bispectral density estimate was obtained for each realization and both the real and imaginary components recorded at the peak frequency along with the magnitude bispectral density peak height. The variance for both real and imaginary components was then estimated and the resulting values averaged to give $\hat{\sigma}^2$. The mean estimated peak value $|\hat{\bar{B}}(\omega_1, \omega_2)|^2$ (which, of course, includes the bias term b), along with $\hat{\sigma}^2$ was then used to estimate the distributions given by Eq. (17). Results were obtained under the null hypothesis ($k_2 = c_2 = 0$) and for varying values of the two nonlinearity parameters.

Sample results are shown in Fig. 3 for the single degree-of-freedom system with a stiffness nonlinearity. Plotted are the distributions of the estimated magnitude auto-bispectral density (normalized) at the peak frequency under the null hypothesis (no nonlinearity) and the alternative (nonlinearity present, $k_2 = 10000$ N/m^2). These results are given for both theory (Fig. 3a) and estimate (Fig. 3b). Results show good agreement between observed and predicted values. Fig. 3c compares both the theoretical and observed

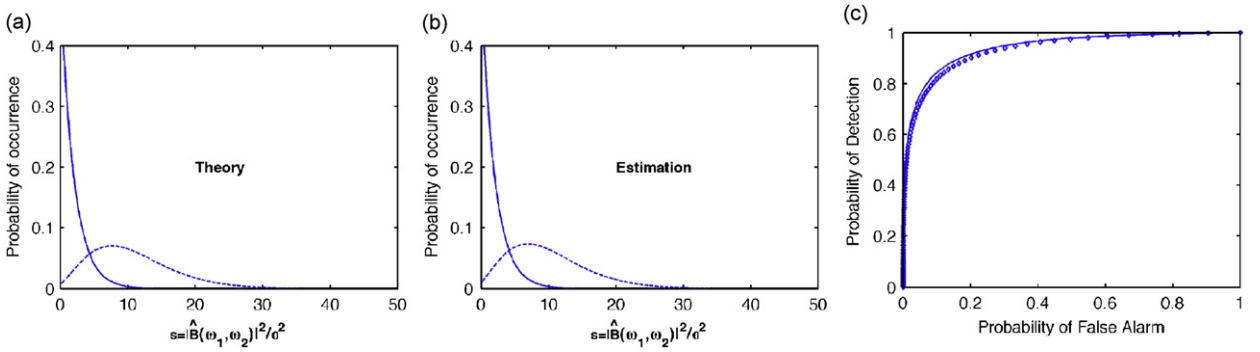

Fig. 3. (a) Peak distributions obtained from theory and (b) those estimated from simulation. The solid line in both (a) and (b) represents the situation where no nonlinearity is present while the dashed line corresponds to a nonlinear stiffness value of $k_2 = 10,000\,\mathrm{N/m^2}$ and no nonlinear damping term ($c_2 = 0\,\mathrm{N\,s^2/m^2}$). The ROC curves associated with theory (solid line) and estimate (diamonds) are shown in (c).

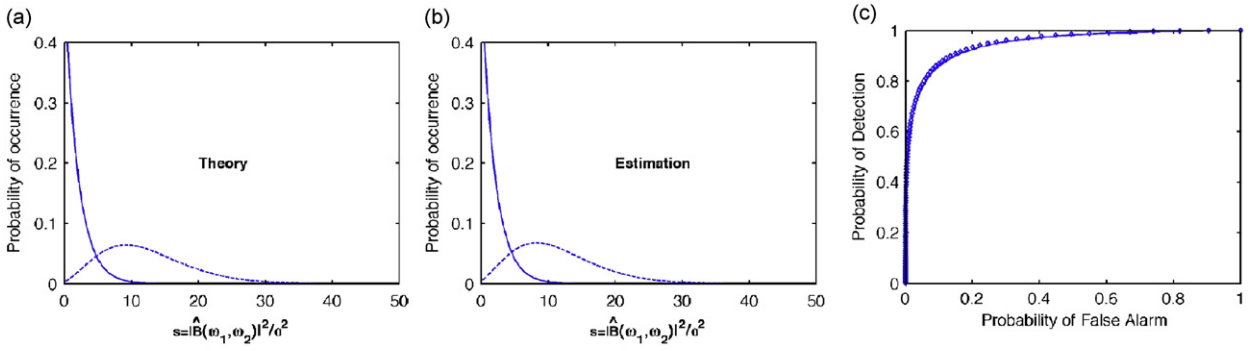

Fig. 4. (a) Peak distributions obtained from theory and (b) those estimated from simulation. The solid line in both (a) and (b) represents the situation where no nonlinearity is present while the dashed line corresponds to a nonlinear damping value of $c_2 = 10\,\mathrm{N\,s^2/m^2}$ and no nonlinear stiffness term ($k_2 = 0\,\mathrm{N/m^2}$). The ROC curves associated with theory (solid line) and estimate (diamonds) are shown in (c).

detector performance in the form of ROC curves. The agreement in the estimated and predicted distributions translates directly into close agreement in the estimated and predicted ROC curves.

The results associated with detecting nonlinear damping are shown in Fig. 4. Again the theory is still able to make good predictions regarding what levels of nonlinearity one can expect to detect and with what probability. Both Type-I and Type-II error are correctly identified.

Finally, the complete set of detection results for both stiffness and damping nonlinearities are shown. Figs. 5 and 6 show the family of ROC curves obtained for varying values of the nonlinearity parameters. For Fig. 5 the nonlinear damping term was set equal to zero ($c_2 = 0$) while the nonlinear stiffness was allowed to vary from 0 to $20,000\,\mathrm{N/m^2}$ in increments of $1000\,\mathrm{N/m^2}$. Conversely, in Fig. 6 the stiffness was zero ($k_2 = 0$) while the nonlinear damping coefficient was varied from 0 to $20\,\mathrm{N\,s^2/m^2}$ in increments of $1\,\mathrm{N\,s^2/m^2}$. In both cases good agreement between estimated and theoretically predicted ROC curves is observed. In the case of varying k_2, both theory and simulation predict that the smallest nonlinearity for which one can obtain 95% POD for 5% PFA is $\sim 13,000\,\mathrm{N/m^2}$ (specifically $13,470\,\mathrm{N/m^2}$). Similarly, it can be seen from theory that a damping value of $c_2 = 13.17\,\mathrm{N\,s^2/m^2}$ allows 95% POD for 5% PFA. Nearly the exact same Type-I and Type-II error were obtained in simulation for this level of damping. It is also important to keep in mind that these results are dependent on the excitation level, P. These results were obtained for $P = 0.01$ [$\mathrm{N^2/Hz}$]. Larger P values will result in being able to detect smaller values of both k_2, c_2. However, it should be mentioned that if both the nonlinearity and excitation levels become large, the two term Volterra model given here may break down and higher-order terms may need to be considered. Again, for detection applications the interest is in small levels of nonlinearity for which the two-term model is appropriate. The model presented here, combined with the statistical properties of the estimates, makes it easy to explore the influence of excitation.

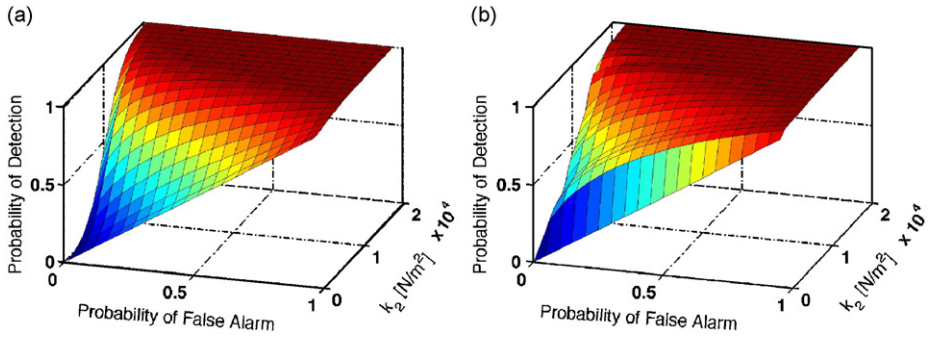

Fig. 5. Comparison of ROC curves generated from theory (a) and simulation (b) as a function of the nonlinearity parameter k_2 N/m^2 ($c_2 = 0$ N s^2/m^2).

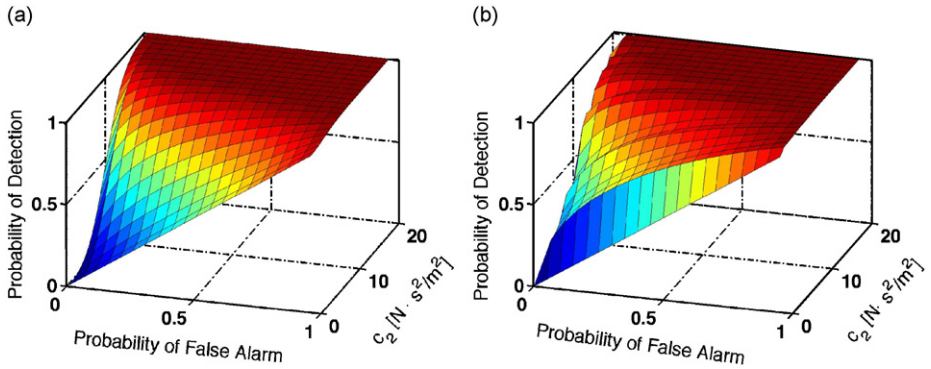

Fig. 6. Comparison of ROC curves generated from theory (a) and simulation (b) as a function of the nonlinearity parameter c_2 N s^2/m^2 ($k_2 = 0$ N/m^2).

It should also be pointed out that for very low levels of nonlinearity the ROC curves associated with the simulation appear to give higher detection probabilities than those obtained from theory. The reason for this is an inability to generate a truly Gaussian time series in practice. In reality there is always some skewness to the driving time series. This skewness results in peaks that, although small, can be detected, even under the null hypothesis of a linear structure. Thus, for small levels of nonlinearity the estimated ROC curves do not exhibit the smooth transition toward the diagonal line predicted by theory for $c_2 = k_2 = 0$.

5. Conclusions

This work has considered both Type-I and Type-II error associated with using the auto-bispectral density, estimated via the direct method, to detect the presence of quadratic nonlinearities in both stiffness and damping. First, an analytical solution for the auto-bispectral density was summarized. Next, an expression for the bias of the estimator was derived. This expression, combined with previously derived expressions for the variance of the estimator, was then used to derive the distributions for the magnitude bispectral density peak height. These distributions allowed for both Type-I and Type-II error to be solved for analytically for the auto-bispectral density-based detector. Receiver operating characteristic (ROC) curves were then used to display these errors in detecting both damping and stiffness nonlinearities. Results were compared to those obtained via numerical simulation and showed good agreement. These results focus only on the uncertainty due to errors in the estimation. In this sense the ROC curves presented show the fundamental limits of auto-bispectral density-based detector performance for single degree-of-freedom systems with quadratic nonlinearities using the direct method of estimation.

References

[1] A.M. Richardson, W.S. Hodgkiss, Bispectral analysis of underwater acoustic data, *Journal of the Acoustical Society of America* 96 (1994) 828–837.

[2] M. Schetzen, *The Volterra and Wiener Theories of Nonlinear Systems*, Wiley, New York, 1980.

[3] P.L. Brockett, M.J. Hinich, D. Patterson, Bispectral-based tests for the detection of gaussianity and linearity time series, *Journal of the American Statistical Association* 83 (1988) 657–664.

[4] K. Worden, G.R. Tomlinson, Nonlinearity in experimental modal analysis, *Philosophical Transactions of the Royal Society A* 359 (2001) 113–130.

[5] A.R. Messina, V. Vittal, Assessment of nonlinear interaction between nonlinearly coupled modes using higher order spectra, *IEEE Transactions on Power Systems* 20 (2005) 375–383.

[6] A. Rivola, P.R. White, Bispectral analysis of the bilinear oscillator with application to the detection of cracks, *Journal of Sound and Vibration* 216 (1998) 889–910.

[7] G.C. Zhang, J. Chen, F.C. Li, W.H. Li, Extracting gear fault features using maximal bispectrum, *Key Engineering Materials* 293–294 (2005) 167–174.

[8] K.K. Teng, J.A. Brandon, Diagnostics of a system with an interface nonlinearity using higher order spectral estimators, *Key Engineering Materials* 204-2 (2001) 271–285.

[9] M.J. Hinich, G.R. Wilson, Detection of non-gaussian signals in non-gaussian noise using the bispectrum, *IEEE Transactions on Acoustics, Speech, and Signal Processing* 38 (1990) 1126–1131.

[10] P. Marzocca, J.M. Nichols, M. Seaver, S.T. Trickey, A. Milanese, Development of higher-order spectra for randomly excited quadratic nonlinear systems: Volterra functional series approach, *Proceedings of the SPIE, Health Monitoring and Smart Nondestructive Evaluation of Structural and Biological Systems VI*, Vol. 6532, SPIE Optical Engineering Press, Bellingham, WA, 2007.

[11] K. Worden, G.R. Tomlinson, *Nonlinearity in Structural Dynamics*, Institute of Physics Publishing, Bristol, UK; Philadelphia, USA, 2001.

[12] E. Bedrosian, S.O. Rice, The output properties of volterra systems (nonlinear systems with memory) driven by harmonic and gaussian inputs, *Proceedings of the IEEE* 59 (1971) 1688–1707.

[13] M.D. Greenberg, *Advanced Engineering Mathematics*, Prentice-Hall, Inc., Englewood Cliffs, NJ, 1988.

[14] C.L. Nikias, M.R. Raghuveer, Bispectrum estimation: a digital signal processing framework, *Proceedings of the IEEE* 75 (1987) 869–891.

[15] K. Sasaki, T. Sato, Y. Yamashita, Minimum bias windows for bispectral estimation, *Journal of Sound and Vibration* 40 (1975) 139–148.

[16] J.S. Bendat, A.G. Piersol, *Random Data Analysis and Measurement Procedures*, third ed., Wiley, New York, 2000.

[17] D.R. Brillinger, M. Rosenblatt, Asymptotic theory of estimates of kth order spectra, in: B. Harris (Ed.), *Advanced Seminar on Spectral Analysis of Time Series*, Wiley, New York, 1967, pp. 153–188.

[18] P.J. Huber, B. Kleiner, T. Gasser, G. Dumermuth, Statistical methods for investigating phase relations in stationary stochastic processes, *IEEE Transactions on Audio and Electroacoustics* AU-19 (1971) 78–86.

[19] R.N. McDonough, A.D. Whalen, *Detection of Signals in Noise*, second ed., Academic Press, San Diego, 1995.